

Local Heating in Nanoscale Conductors

Yu-Chang Chen, Michael Zwolak, and Massimiliano Di Ventra*

*Department of Physics, Virginia Polytechnic Institute and State University,
Blacksburg, Virginia 24061**Received October 2, 2003*

ABSTRACT

We report first-principles calculations of local heating in nanoscale junctions formed by a single molecule and a gold point contact. Due to the lower current density and larger heat dissipation, the single molecule heats less than the gold point contact. We also find that, at zero temperature, threshold biases, V_{onset} , of about 6 mV and 11 mV for the molecule and the point contact, respectively, are required to excite the smallest vibrational mode and generate heat. The latter estimate is in very good agreement with recent experimental results on the same system. At a given external bias V below V_{onset} , heating becomes noticeable when the background temperature is on the order of approximately $e(V_{\text{onset}} - V)/k_B$. Above V_{onset} , local heating increases dramatically with increasing bias, mainly due to excitation of longitudinal modes, but is also considerably suppressed by thermal dissipation into the electrodes, provided good thermal contacts exist between the nanostructure and the bulk electrodes.

Local heating occurs when electrons diffusing in a conductor release energy to the ions via scattering with phonons. The amount of heat generated in a given portion of the conductor depends on several factors: the strength of the electron–phonon interaction, the current density, the background temperature, and the inelastic electron mean free path. In a nanoscale junction, the inelastic electron mean free path is large compared to the dimensions of the junction. As a consequence, each electron releases only a small fraction of its energy during the time it spends in the junction.^{1,2} However, there can still be substantial local heating due to the large current density in nanoscale junctions. Indeed, such an effect has been observed in several atomic-scale structures.^{3–9} Apart from its fundamental importance in solid state physics, the problem has thus gained renewed interest due to its possible impact on nanoscale electronics. At this length scale, all atoms of the junction and corresponding vibrational modes need to be treated explicitly, and the electronic distribution calculated self-consistently with the correct scattering boundary conditions. Only a few theoretical investigations, mainly using the tight-binding approximation, have tackled this problem at the atomic level.^{1,2,10–14}

In this letter, we derive a general expression for the power transferred by the electrons to the vibrational modes of a nanoscale junction and calculate the local heating using first-principles approaches. Combined with a model of heat transfer to the electrodes, the approach provides a microscopic and detailed picture of current-induced heat generation in nanoscale conductors. As an example, we discuss local heating for a single molecule between gold electrodes and a gold point contact. We find that the single-

molecule junction heats less than the gold point contact due to a larger heat dissipation into the electrodes and larger resistance to electron flow. In the case of the gold point contact, experimental data is available which is in good agreement with the predicted threshold bias, V_{onset} , for heat generation and corresponding local temperature.^{5,9} At a given external bias V below V_{onset} , we find that local heating becomes noticeable when the background temperature is larger than approximately $e(V_{\text{onset}} - V)/k_B$, but is also considerably suppressed by thermal dissipation into the electrodes.

Let us start by considering a nanoscale structure between two bulk electrodes. The many-body Hamiltonian of the system is

$$H = H_{\text{el}} + H_{\text{ion}} + H_{\text{el-ion}} \quad (1)$$

where H_{el} is the electronic Hamiltonian, $H_{\text{ion}} = \sum_{i=1}^N \mathbf{P}_i^2 / 2M_i + \sum_{i<j} V_{\text{ion}}(\mathbf{R}_i - \mathbf{R}_j)$ is the ionic Hamiltonian, and $H_{\text{el-ion}} = \sum_{i,j} V_{\text{el-ion}}(\mathbf{r}_i - \mathbf{R}_j)$ describes the electron–ion interaction. \mathbf{R}_i , \mathbf{P}_i , and M_i are the coordinates, momentum, and mass, respectively, of the i th ion; \mathbf{r}_i is the coordinate of the i th electron. In the adiabatic approximation, the Hamiltonian (eq 1) has effective single-particle wave functions $\Psi_E^{L(R)}(\mathbf{r}, \mathbf{K}_{\parallel})$ with energy E and momentum \mathbf{K}_{\parallel} parallel to the electrode surface, corresponding to electrons incident from the left (right) electrodes.¹⁵ We calculate these single-particle wave functions, in the absence of electron–vibration coupling, using a scattering approach within the density functional theory of many-electron systems.¹⁵

To calculate the electron–phonon interaction, we consider a small deviation $\mathbf{Q}_i = \mathbf{R}_i - \mathbf{R}_i^0$ of the i th ion from its

* Corresponding author. E-mail address: diventra@vt.edu.

equilibrium position \mathbf{R}_i^0 . We introduce normal coordinates $\{q_{i\mu}\}$ such that the μ th component ($\mu = x, y, z$) of \mathbf{Q}_i is

$$(\mathbf{Q}_i)_\mu = \sum_{j=1}^N \sum_{\nu=1}^3 A_{i\mu,j\nu} q_{j\nu} \quad (2)$$

The transformation matrix, $\mathbf{A} = \{A_{i\mu,j\nu}\}$, satisfies the orthonormality relations: $\sum_{i,\mu} M_i A_{i\mu,j\nu} A_{i\mu,j'\nu'} = \delta_{j\nu,j'\nu'}$. The Hamiltonian describing the ionic vibrations can then be decoupled into a set of independent harmonic oscillators:

$$H_{\text{vib}} = \frac{1}{2} \sum_{i,\mu \in \text{vib}} \dot{q}_{i\mu}^2 + \frac{1}{2} \sum_{i,\mu \in \text{vib}} \omega_{i\mu}^2 q_{i\mu}^2 \quad (3)$$

where $\{\omega_{i\mu}\}$ are the normal-mode frequencies and the summations are carried out for all normal modes. We calculate these modes from first-principles.¹⁶

We now introduce the field operator, $\hat{\Psi} = \hat{\Psi}^L + \hat{\Psi}^R$, which describes electrons incident from the left (L) and right (R) electrodes, where¹⁷

$$\hat{\Psi}^{L(R)} = \sum_E a_E^{L(R)} \Psi_E^{L(R)}(\mathbf{r}, \mathbf{K}_{\parallel}) \quad (4)$$

The coefficients $a_E^{L(R)}$ are the annihilation operators for electrons incident from the left (right) electrode. They satisfy the usual anticommutation relations $\{a_E^i, a_{E'}^{j\dagger}\} = \delta_{ij} \delta(E - E')$. We also assume that the electrons rapidly thermalize into the bulk electrodes so that their statistics are given by the equilibrium Fermi–Dirac distribution, $f_E^{L(R)} = 1/(\exp[(E - E_{\text{FL(R)}})/k_B T_e] + 1)$, in the left (right) electrodes, where T_e is the background temperature.

We can now express $(\mathbf{Q}_i)_\mu$ in terms of boson annihilation and creation operators. Together with the field operator $\hat{\Psi}$, the second-quantized form of H_{vib} and the electron–vibration interaction, $H_{\text{el–vib}}$, can be written as

$$H_{\text{vib}} = \sum_{j\nu \in \text{vib}} \left(b_{j\nu}^\dagger b_{j\nu} + \frac{1}{2} \right) \hbar \omega_{j\nu} \quad (5)$$

and

$$H_{\text{el–vib}} = \sum_{\alpha,\beta} \sum_{E_1, E_2} \sum_{i\mu, j\nu \in \text{vib}} \sqrt{\frac{\hbar}{2\omega_{j\nu}}} A_{i\mu, j\nu} J_{E_1, E_2}^{i\mu, \alpha\beta} a_{E_1}^{\alpha*} a_{E_2}^\beta (b_{j\nu} + b_{j\nu}^\dagger) \quad (6)$$

where $\alpha, \beta = L, R$; $i, j = 1, \dots, N$; and $\mu, \nu = 1, 2, 3$. The quantity $J_{E_1, E_2}^{i\mu, \alpha\beta}$ is the electron–vibration coupling constant and has the form

$$J_{E_1, E_2}^{i\mu, \alpha\beta} = \int d\mathbf{r} \int d\mathbf{K}_{\parallel} \Psi_{E_1}^{\alpha*}(\mathbf{r}, \mathbf{K}_{\parallel}) \partial_\mu V^{ps}(\mathbf{r}, \mathbf{R}_i) \Psi_{E_2}^\beta(\mathbf{r}, \mathbf{K}_{\parallel}) \quad (7)$$

where we have chosen to describe the electron–ion interaction with pseudopotentials $V^{ps}(\mathbf{r}, \mathbf{R}_i)$ for each i th ion.¹⁵ The terms $b_{j\nu}$ are the annihilation operators for the $j\nu$ th vibrational

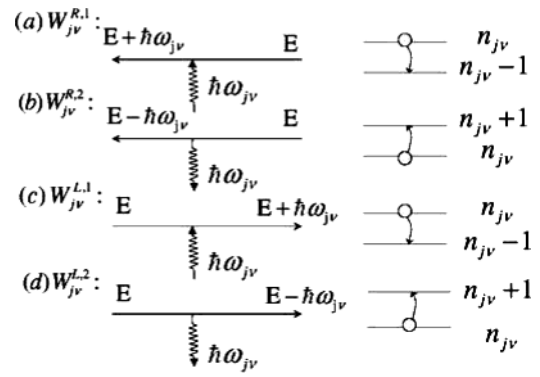


Figure 1. Feynman diagrams of the four main electron–phonon scattering mechanisms contributing to local heating of the junction. (a) Cooling process due to absorption of a phonon from a left-moving electron. (b) Heating process due to the emission of a phonon from a left-moving electron. (c) and (d) are the equivalent mechanisms corresponding to the right-moving electrons.

modes and satisfy the commutation relation $[b_{j\nu}, b_{j'\nu'}^\dagger] = \delta_{j\nu, j'\nu'}$. The statistics of these modes are described by the Bose–Einstein distribution:

$$\langle b_{j\nu}^\dagger b_{j'\nu'} \rangle = \delta_{j\nu, j'\nu'} / \exp[(n_{j\nu} + 1/2)\hbar\omega_{j\nu}/k_B T_w - 1] \quad (8)$$

where T_w is the local temperature of the junction.

For each normal mode, we can now calculate the rates of thermal energy generated by the electron–vibration interactions corresponding to the first-order processes described in Figure 1. These processes correspond to electrons incident from the right or left electrode that absorb (cooling) or emit (heating) energy because of the electron–vibration scattering. We evaluate these rates with the Fermi golden rule

$$W_{j\nu}^{R,k} = 2\pi\rho(\delta_{k,2} + \langle n(n_{j\nu}) \rangle) \int dE \left| \sum_{i\mu} A_{i\mu, j\nu} J_{E \pm \hbar\omega_{j\nu}, E}^{i\mu, LR} \right|^2 \times f_E^R (1 - f_{E \pm \hbar\omega_{j\nu}}^L) D_{E \pm \hbar\omega_{j\nu}}^L D_E^R \quad (9)$$

$$W_{j\nu}^{L,k} = W_{j\nu}^{R,k} (R \rightleftharpoons L) \quad (10)$$

where $R \rightleftharpoons L$ means interchange of labels R and L; the positive (negative) sign in eq 9 is for $k = 1(2)$, corresponding to relaxation (excitation) of vibrational modes; $D_E^{L(R)}$ is the partial density of states corresponding to $\Psi_E^{L(R)}$, whose sum is the total density of states. The term $\delta_{k,2}$ corresponds to spontaneous emission. Finally, a factor of 2 due to spin degeneracy appears in eq 9.¹⁸

Because electrons can excite all possible energy levels of a mode with frequency $\omega_{j\nu}$, the statistical average $\langle n(n_{j\nu}) \rangle$ is required. The total thermal power generated in the junction is therefore the sum over all vibrational modes for the four processes of Figure (1):

$$P = \sum_{j\nu \in \text{vib}} (W_{j\nu}^{R,2} + W_{j\nu}^{L,2} - W_{j\nu}^{R,1} - W_{j\nu}^{L,1}) \quad (11)$$

Equation 11 is the central result of this paper. It allows for a first-principles calculation of the local temperature in a

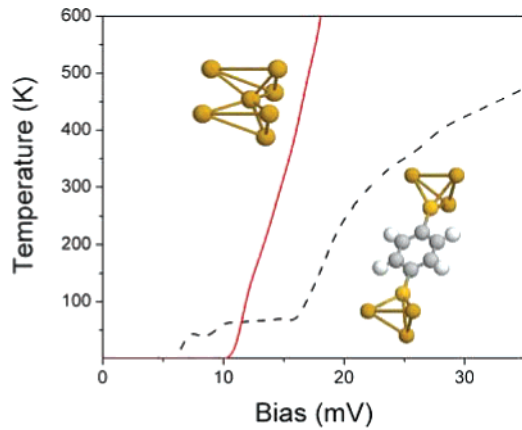


Figure 2. Local equilibrium temperature as a function of bias for a benzene–dithiolate molecular junction (dashed line, schematic in the right-lower corner) and a single-gold-atom point contact (solid line, schematic in the left-upper corner) at $T_e = 0$ K. No heat dissipation into the electrodes is taken into account.

nanoscale junction. It is similar to the expression obtain by Montgomery et al. within a tight-binding approach.² We now discuss results for two specific cases: local heating in a benzene–dithiolate molecular junction and a gold point contact (see schematics in Figure 2). We also assume the left electrode to be positively biased. At zero temperature (i.e., $T_e = 0$ and $T_w = 0$), the heating processes $\{W_{jv}^{L,2}\}$, corresponding to electrons incident from the left electrode, vanish due to the Pauli exclusion principle; the cooling processes $\{W_{jv}^{R,1}\}$ and $\{W_{jv}^{L,1}\}$, corresponding to the transitions from a high to a low energy level of the modes, are also prohibited because all modes are at the ground state. The only nonzero contribution to local heating is therefore from $W_{jv}^{R,2}$, i.e.,

$$P = 2\pi\hbar \sum_{jv \in vib} (1 + \langle n(n_{jv}) \rangle) \int_{E_{FR}}^{E_{FL} + \hbar\omega_{jv}} dE | \sum_{i\mu} A_{i\mu,jv} J_{E-\hbar\omega_{jv},E}^{i\mu,LR} | \times D_{E-\hbar\omega_{jv}}^L D_E^R \quad (12)$$

A bias greater than $V_{\text{onset}} = \min\{\hbar\omega_{jv}\}/e$ is therefore necessary to generate heat. The smallest vibrational frequency calculated from first principles¹⁶ is about 6 mV and 11 mV for the molecule and the point contact, respectively. The latter estimate is in very good agreement with recent experimental observations.⁹ When the bias is smaller than the threshold voltage, local heating is possible only at nonzero background temperature T_e . This is caused by a small fraction of thermally excited electrons that can induce level transitions of the normal modes. The heating generated is substantial when $k_B T_e \approx \min\{\hbar\omega_{jv}\} - (E_{FR} - E_{FL})$.

At $T_e = 0$ and $T_w > 0$, the junction heats progressively, and eventually an equilibrium temperature is reached when the heating processes ($W_{jv}^{R,2}$ and $W_{jv}^{L,2}$) balance the cooling processes ($W_{jv}^{R,1}$ and $W_{jv}^{L,1}$). The corresponding local equilibrium temperature is plotted in Figure 2 for both the single molecule junction and the gold point contact. It is evident from Figure 2 that the equilibrium temperature increases abruptly above the threshold voltage, and it is

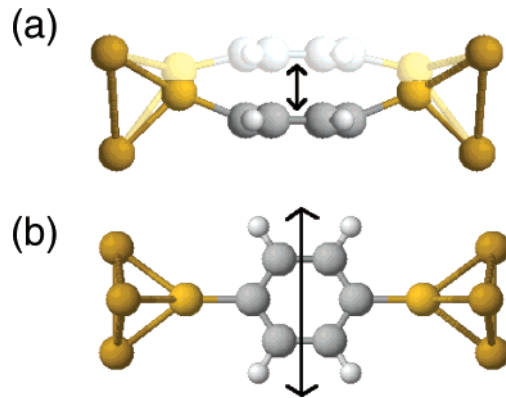


Figure 3. The two modes contributing to heating at $T_e = 0$ and $V < 10$ mV. (a) The vibrational mode with energy $\hbar\omega \approx 6$ meV. (b) The mode with energy $\hbar\omega \approx 9$ meV.

already substantial at biases of only few mV. The reason for this dramatic increase resides again in quantum statistics which favor the heating processes.

In the case of the gold point contact, the longitudinal vibrational mode of the single gold atom ($\hbar\omega \approx 11.5$ meV) contributes the most to the local heating above $V = 11.5$ mV, even though the two transverse modes have slightly smaller frequencies ($\hbar\omega \approx 10.8$ meV) and are excited at a lower bias. In linear response ($V < 10$ mV), two modes contribute to local heating in the case of the single-molecule junction (see Figure 3). One, with energy $\hbar\omega \approx 6$ meV, corresponds to the central benzene ring moving up and down with respect to its equilibrium position (Figure 3a). The second, with energy $\hbar\omega \approx 9$ meV, corresponds to the central ring moving sideways with respect to its equilibrium position (Figure 3b). The first mode contributes to local heating much more than the second one, as determined by the transformation matrix $A_{i\mu,jv}$ and phonon coupling (eq 7). At a bias of about 0.5 V, all vibrational modes of the molecular junction are excited. The mode that contributes the most to heating corresponds to an in-plane “breathing” of the central carbon ring (not shown).¹⁹ In general, longitudinal modes give larger contribution to heating than transverse modes.

So far we have assumed the junction is thermally isolated. However, the majority of the heat generated in the junction is actually transferred to the electrodes. We estimate the thermal conductance following the approach of Patton and Geller.^{20,21} We assume the junction to be a weak thermal link with a given stiffness K , which we evaluate from first principles.²² We then estimate the thermal current into the electrodes via elastic phonon scattering as²⁰

$$I_{\text{th}} = \frac{4\pi K^2}{\hbar} \int d\epsilon \epsilon N_L(\epsilon) N_R(\epsilon) [n_L(\epsilon) - n_R(\epsilon)] \quad (13)$$

where $n_{L(R)}$ is the Bose–Einstein distribution function, $N_{L(R)}(\epsilon)$ is the spectral density of states at the left (right) electrode surface, and $K = \pi d^2 Y / (4l)$. Y is the Young’s modulus of the junction, and d (l) is its diameter (length).²⁰ We note that the temperature profile along a nanojunction is nearly constant and almost equal to the average temper-

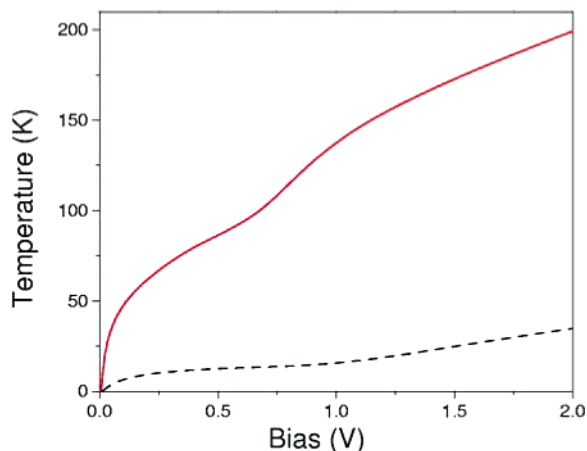


Figure 4. Local temperature as a function of bias for a benzene–dithiolate molecular junction (dashed line) and a gold point contact (solid line) due to the equilibrium between local heating and heat dissipation into the electrodes at $T_e = 0$ K.

ature of the thermal reservoirs.²³ The thermal current from the junction with temperature T_w dissipated to the left electrode with temperature T_e is thus equivalent to the thermal current of a weak thermal link between reservoirs with temperatures T_e and $2T_w - T_e$. Analogously for the thermal current into the right electrode. The effective local temperature, resulting from the equilibrium between local heating and heat dissipation into the electrodes, is plotted in Figure 4 at $T_e = 0$ K. Values of the local temperature for the gold contact are in good agreement with experimental results⁵ and previous theoretical estimates.¹

It is evident from Figure 4 that the local temperature is considerably reduced by heat transfer into the electrodes even for relatively large biases (cf. Figure 2). It is also evident that at any given bias the single-molecule junction heats less than the gold point contact. This is due to the larger stiffness of the molecule ($K_{\text{molecule}} = 6.7 \times 10^4$ erg/cm², $K_{\text{gold}} = 9.4 \times 10^3$ erg/cm²), and its larger resistance to electrical current (the calculated gold point contact conductance is about $1.1 2e^2/h$ independent of bias, while the molecule has a conductance of about $0.04 2e^2/h$ at 0.01 V and changes nonlinearly with bias¹⁵).

It is clear from the above results that good thermal contacts are necessary in order to have efficient dissipation of heat into the electrodes. Without such good thermal contacts, very high local temperatures can be easily generated at very low biases, which would lead to structural instabilities of the nanostructure.

Acknowledgment. We thank T. N. Todorov for useful discussions. We acknowledge support from the NSF Grant Nos. DMR-01-02277 and DMR-01-33075, and Carilion

Biomedical Institute. Acknowledgment is also made to the donors of the Petroleum Research Fund, administered by the American Chemical Society, for partial support of this research.

References

- (1) Todorov, T. N. *Philos. Mag. B* **1998**, *77*, 965.
- (2) Montgomery, M. J.; Todorov, T. N.; Sutton, A. P. *J. Phys.: Condens. Mater.* **2002**, *14*, 1. Montgomery, M. J.; Hoekstra, J.; Todorov, T. N.; Sutton, A. P. *J. Phys.: Condens. Mater.* **2003**, *15*, 731.
- (3) Yanson, I. K. *Sov. Phys. JETP* **1974**, *39*, 506.
- (4) Muller, C. J.; van Ruitenbeek, J. M.; deJongh, J. L. *Phys. Rev. Lett.* **1992**, *69*, 140.
- (5) van den Brom, H. E.; Yanson, A. I.; van Ruitenbeek, J. M. *Physica B* **1998**, *252*, 69.
- (6) van Gelder, A. P.; Jansen, A. G. M.; Wyder, P.; *Phys. Rev. B* **1980**, *22*, 1515.
- (7) Persson, B. N. J.; Avouris, Ph. *Surf. Sci.* **1997**, *390*, 45.
- (8) Lorente, N.; Persson, M.; Lauhon, L. J.; Ho, W. *Phys. Rev. Lett.* **2001**, *86*, 2593.
- (9) Agrait, N.; Untiedt, C.; Rubio-Bollinger, G.; Vieira, S. *Phys. Rev. Lett.* **2002**, *88*, 216803.
- (10) Ness, H.; Fisher, A. J. *Phys. Rev. Lett.* **1999**, *83*, 452.
- (11) Troisi, A.; Ratner, M. A.; Nitzan, A. *J. Chem. Phys.* **2003**, *118*, 6072.
- (12) D'Amato, J. L.; Pastawski, H. M. *Phys. Rev. B* **1990**, *41*, 7411.
- (13) Bonca, J.; Trugman, S. A. *Phys. Rev. Lett.* **1995**, *75*, 2566.
- (14) Emberly, E. G.; Kirczenow, G. *Phys. Rev. B* **2000**, *61*, 5740.
- (15) Lang, N. D. *Phys. Rev. B* **1995**, *52*, 5335. Di Ventra, M.; Lang, N. D. *Phys. Rev. B* **2002**, *65*, 045402. Yang, Z.; Tackett, A.; Di Ventra, M. *Phys. Rev. B* **2002**, *66*, 041405. Di Ventra, M.; Pantelides, S. T.; Lang, N. D. *Phys. Rev. Lett.* **2000**, *84*, 979.
- (16) We have employed Hartree–Fock total energy calculations [see, e.g., Boatz, J. A.; Gordon, M. S. *J. Phys. Chem.* **1989**, *93*, 1819] to evaluate the vibrational modes of the single-molecule junction and the gold point contact. For these calculations, the assumed surface geometry is (111), represented by a triangular pad of gold atoms (see insets of Figure 2) with infinite mass. Both S atoms and the single gold atom face the center of the triangular pad. The chosen S-surface distance is 2.4 Å, the single gold-surface distance is 2.3 Å. Another configuration for the molecule, e.g., the S atom facing a single gold atom of the surface, would give lower current¹⁵ and thus lower local heating.
- (17) Chen, Y.-C.; Di Ventra, M. *Phys. Rev. B* **2003**, *67*, 153304.
- (18) The inelastic electron mean-free path estimated from the Fermi golden rule is at least 100 Å, in agreement with estimates reported in ref 2.
- (19) Di Ventra, M.; Pantelides, S. T.; Lang, N. D. *Phys. Rev. Lett.* **2002**, *88*, 046801.
- (20) Patton, K. R.; Geller, M. R. *Phys. Rev. B* **2001**, *64*, 155320.
- (21) The present model provides an intuitive picture of the heat transfer from the junction to the electrodes with some details of the link between the two bulk reservoirs. Note, however, that similar conclusions would be reached if we used, e.g., a semiclassical model of heat conduction as done in ref 1.
- (22) The following parameters have been used: Young's modulus of the gold contact, 5.0×10^{11} dyn/cm² [from Kracke, B.; Damaschke, B. *Appl. Phys. Lett.* **2000**, *77*, 361]; Young's modulus of the benzene–dithiolate molecule, 52.6×10^{11} dyn/cm² (estimated from total energy calculations); gold contact effective diameter, 4.6 a.u.; molecule effective diameter 6.9 a.u. The spectral densities $N_{L(R)}(\epsilon)$ are estimated according to ref 20, with longitudinal and transverse sound velocities for bulk gold, $v_l = 3.2 \times 10^5$ cm/s and $v_t = 1.2 \times 10^5$ cm/s, respectively.
- (23) See, e.g., Zürcher, U.; Talkner, P. *Phys. Rev. A* **1990**, *42*, 3278.

NL0348544